DOI: 10.1002/chem.200601756

An Anthracene-Appended β-Cyclodextrin-Based Dyad: Study of Self-Assembly and Photoinduced Electron-Transfer Processes

Bijitha Balan and Karical R. Gopidas*[a]

Abstract: The self-assembly of a β-cyclodextrin (β-CD)-based supramolecular dyad is reported, in which the donor anthracene moiety is covalently linked to the smaller rim of the β-CD and the acceptor pyromellitic diimide (PMDI) is encapsulated within the β-CD cavity. Encapsulation of the PMDI into the β-CD cavity was studied by a variety of techniques, which suggested that PMDI is encapsulated so as to position the aromatic part at the centre of the cavity with the 2-propyl end at the narrower rim among the overhanging primary OH groups and the *N*-ethylpyridinium end situated at the wider rim exposed to water. Photoinduced electron transfer (PET) in the system was studied by fluorescence quenching and laser flash photolysis techniques. At $[PMDI] < 10^{-4}$ M, the equilibrium is in favour of the free molecules, and under these conditions fluorescence quenching is negligible and diffusion-mediated electron transfer involving the triplet excited state of anthracene predominates. At higher concentrations of PMDI, the equilibrium is largely in favour of the supramolecular dyad and intra-ensemble PET processes predominate. The experimentally determined electron-transfer rate constant agrees very well with that calculated by using the Marcus equation. It was observed that a fraction of the ion pairs survived for more than 200 μs.

Keywords: cyclodextrins · donor–acceptor systems · electron transfer · flash photolysis · fluorescence

Introduction

The construction of supramolecular donor–acceptor systems for photoinduced energy- and electron-transfer processes has gained considerable importance in the last few years.[1] Hydrogen bonding, π stacking and metal–ligand coordination are the non-covalent interactions often exploited for the design of supramolecular assemblies. These interactions, however, are not very effective for designing water-soluble supramolecular systems. Cyclodextrins (CDs), which are cyclic oligosaccharides with hydrophobic cavities, are ideal molecular receptors for building water-soluble supramolecular functional systems.[2] The commonly available CDs, namely α-, β- and γ-CDs, have six, seven or eight D-glucopyranose units, respectively, linked by α-(1,4) linkages. CDs are shaped like truncated cones with the primary hydroxyl groups of the glucose units arranged on the narrow rim and the secondary hydroxyl groups assembled on the wider rim. CDs are capable of encapsulating small molecules within their cavities. As a result of their water solubility, guest-encapsulation properties and ability to mimic natural enzymatic systems, CDs are increasingly used in the design of supramolecular electron- and energy-transfer systems. For example, photoinduced electron-transfer (PET) reactions between CD-appended aromatics or metal complexes and encapsulated guest molecules have already been reported.[3] These reports, however, used only steady-state and time-resolved fluorescence techniques, which gave information only about the forward electron-transfer process. Reports dealing with the characterization of the radical-ion intermediates by using laser flash photolysis, and determination of their yields and lifetimes, are very few in number.[3m–q] Herein, some of these issues are addressed.

In a recent publication, we reported the PET reactions between α-CD-appended pyrene and a few acceptor molecules in aqueous solutions.[4] The acceptors were monocyclic aromatic molecules capable of encapsulation in the α-CD cavity. PET processes in these dyads were probed by fluorescence lifetime quenching experiments, which showed that PET reactions in the CD-based dyad systems obey the Marcus equation. Here we report the assembly of a β-CD-

[a] B. Balan, Dr. K. R. Gopidas
Photosciences and Photonics Section
Chemical Sciences and Technology Division
Regional Research Laboratory (CSIR)
Trivandrum 695019 (India)
Fax: (+91) 471-249-1712
E-mail: gopidaskr@rediffmail.com

Supporting information for this article is available on the WWW under http://www.chemeurj.org/ or from the author.

 © 2007 Wiley-VCH Verlag GmbH & Co. KGaA, Weinheim WILEY InterScience DISCOVER SOMETHING GREAT

based supramolecular dyad, wherein an anthracene (AN) moiety covalently attached to the smaller rim of β-CD acts as the donor and a pyromellitic diimide (PMDI) derivative encapsulated within the β-CD cavity acts as the acceptor. Self-assembly of the dyad was studied by absorption, fluorescence and ^{1}H NMR spectroscopy, and by circular dichroism and cyclic voltammetry (CV). PET reactions in the supramolecular dyad were studied by fluorescence quenching and laser flash photolysis. Our results suggest that the design of the supramolecular dyad can result in the formation of a long-lived charge-separated (CS) state in moderate yield.

Results and Discussion

Structural characterization and photophysical properties of β-cyclodextrin-appended anthracene (ANCD): ANCD was synthesized by using a well-known strategy developed for the selective functionalisation of the narrower rim of CDs (Scheme 1).[5] The structure of ANCD is assigned based on spectral evidence (see the Experimental Section). The MALDI-TOF mass spectrum of ANCD, for example, showed a peak at m/z: 1325, which corresponded to $[ANCD+H]^+$ (see the Supporting Information S1). The peak corresponding to native β-CD was not observed in the MALDI-TOF spectrum. The ^{1}H NMR spectrum of ANCD exhibited peaks due to the β-CD part at $\delta = 3.1$–5.9 ppm and the aromatic residue at $\delta = 7.5$–8.6 ppm. The regiochemistry of ANCD was assigned based on a comparison of the ^{13}C NMR chemical shifts (see Supporting Information S2) with those reported for similar compounds. β-CD has seven glucose units and in monosubstituted β-CD systems, the ^{13}C NMR chemical shifts of six of the glucose units remain relatively unaffected by the substitution. The ^{13}C NMR chemical shifts of the AN-attached glucose unit are expected to be modified. D'Souza and co-workers have shown that, if the C_6–OH is substituted, the C_6 carbon shifts downfield by $\delta \approx 10$ ppm, C_5 shifts upfield by $\delta \approx 2$ ppm and C_4 shifts downfield by $\delta \approx 0.5$ ppm.[5a] The ^{13}C NMR spectrum of ANCD exhibited six intense signals and eight small peaks in the carbohydrate region. Based on a comparison with the literature, the six intense signals are assigned to those in the six unsubstituted glucose rings at $\delta = 102.34$ (C_1), 81.57 (C_4), 73.12 (C_3), 72.48 (C_5), 72.09 (C_2) and 59.98 ppm (C_6). The small peak at $\delta = 64.65$ ppm is assigned to the CH_2 group attached to AN. Six of the remaining seven peaks must be due to the six carbon atoms in the AN-attached glucose ring. Of these, the peak at $\delta = 68.85$ ppm is assigned to the C_6 carbon and this signal is $\delta = 8.87$ ppm downfield from the normal value because of attachment to the AN residue. The other signals were: C_5 at $\delta = 70.73$ (1.75 upfield), C_4 at 82.05 (0.48 downfield), C_3 at 73.52 (0.4 downfield), C_2 at 71.8 (0.29 upfield) and C_1 at 102.58 ppm (0.24 ppm downfield). As the C_6 signal is shifted by nearly $\delta = 9$ ppm and C_5 is shifted by $\delta = 1.75$ ppm, we confirm that the AN moiety is attached to the C_6 carbon atom, which is on the narrower rim of β-CD. A small signal at $\delta = 60.31$ ppm remains unaccounted. We assign this to the C_6 carbon atoms of the glucose units adjacent to the one to which AN is attached. (When a relatively large molecule like AN is attached to the narrower rim of β-CD, the CH_2OH groups projecting out of the narrower rim may experience steric crowding. This effect may be more on adjacent glucose rings and hence their chemical shifts may be affected. D'Souza and co-workers also observed such a peak, but they have not assigned it. In a pyrene-attached α-CD, we observed a similar signal and assigned this to the C_6 carbon atoms of adjacent glucose units.)

Details regarding the conformation of ANCD were obtained from UV/visible, fluorescence and circular dichroism studies. The actual conformation is expected to be in between the two extremes, namely, 1) an extended conformation in which the AN moiety is fully stretched out into solution and 2) a folded conformation in which the AN moiety is folded back, so as to become encapsulated fully or partially in the CD cavity. In the extended conformation, the AN residue is fully exposed to water and the spectral characteristics are expected to be similar to those of a water-soluble AN derivative, such as (9-anthrylmethyl)triethylammonium chloride (AMTAC, see the Supporting Information Scheme S3 for structure). Figure 1a shows the absorption spectra of ANCD and AMTAC in water. The absorption spectrum of AN in the relatively non-polar solvent THF (AN/THF) is also shown for comparison. The absorption spectra are characterized by four vibrational bands. The vibrational band maxima in ANCD (334, 350, 368 and 388 nm) are in between the values for AN/THF (326, 342, 360 and 379 nm) and AMTAC in water (338, 355, 373 and 393 nm). The emission spectra of ANCD and AMTAC in water and AN/THF are shown in Figure 1b. When the band maxima are compared, ANCD (391, 412, 436 and 468 nm) appears closer to AMTAC in water (392, 411, 435 and 466 nm) than to AN/THF (382, 402, 373 and 453 nm). The band shapes, however, exhibited some difference. For example, the intensities of the first and

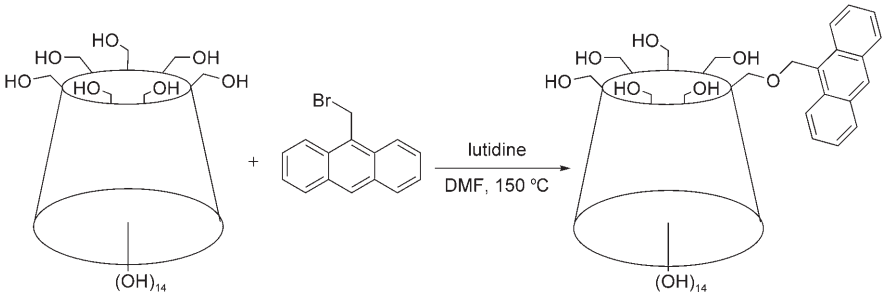

Scheme 1. Synthesis of ANCD.

 © 2007 Wiley-VCH Verlag GmbH & Co. KGaA, Weinheim

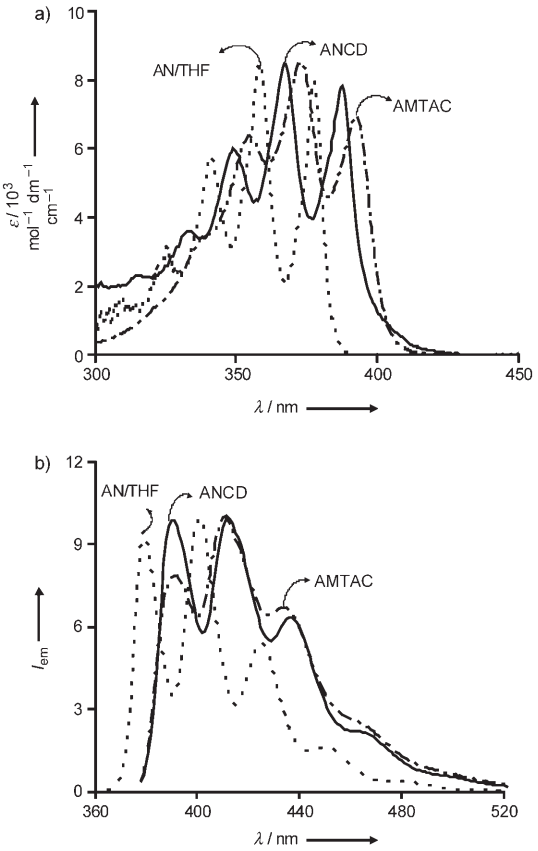

Figure 1. a) Absorption and b) emission spectra of AN in THF (•••••), ANCD in water (——) and AMTAC in water (–•–•–).

second emission bands are comparable in ANCD and AN/THF. In AMTAC the first band is lower in intensity. Thus, the absorption and emission spectra suggest that the AN residue in ANCD is not fully exposed to water.

Further insight into the conformation of ANCD is obtained by using circular dichroism spectroscopy. Achiral molecules included in the CD cavity or attached to the rim of the CD often exhibit induced circular dichroism (ICD) spectra, the sign and intensity of which are very sensitive to the orientation of the achiral molecule. The orientation is usually deduced from ICD spectra by using the rules derived for ICD of chiral supramolecular systems, which were initially derived for CD complexes[6] and then generalized for complexes of chiral macrocycles.[7] The rules predict the following: 1) The sign of ICD is positive for a transition polarized parallel to the axis of the macrocyclic host and negative for that polarized perpendicular to the axis. 2) The sign of ICD is reversed when a chromophore moves from the inside of the host cavity to the outside, while keeping the direction of the transition moment unchanged. 3) The absolute value of ICD is greater when a chromophore exists on the outside of the narrower rim than when it is on the outside of the wider rim. 4) The ICD value of a transition polarized perpendicular to the axis of a macrocycle is $-1/2$ of that of a parallel-polarized one and the sign of ICD changes at 54.7°. These rules were successfully applied for the conformational analysis of several CD-appended chromophores.[8]

The long-wavelength absorption of AN in the 300–400 nm region is polarized along its short axis.[9] The length of the AN molecule is larger than the diameter of β-CD, and hence AN can enter the β-CD cavity only with its long axis parallel to the β-CD axis. In this conformation, the transition moment of the 300–400 nm absorption would be perpendicular to the β-CD axis and one would expect a negative ICD signal. It should be noted that AN is attached to β-CD at the 9-position, and this makes it difficult for complete inclusion of the AN moiety within the cavity.

ANCD in water exhibits a weak negative ICD signal (spectrum A in Figure 2) in the 300–400 nm region. The ICD signal was independent of concentration, suggesting

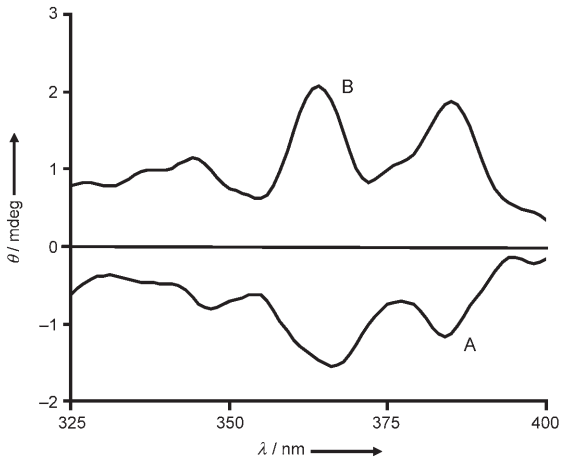

Figure 2. ICD spectrum of ANCD (1.2×10^{-4} M) in water in the absence (A) and presence (B) of ADAC (3×10^{-3} M).

that the signal is due to an intramolecular process. Intermolecular processes such as inclusion of the AN part of one molecule into the β-CD part of another molecule can be ruled out. According to rules 1 and 2 above, negative ICD can result from two orientations: 1) The AN moiety is included within the β-CD cavity with its long axis parallel to the β-CD axis. 2) The AN moiety is held outside the cavity with its long axis perpendicular to the β-CD axis. In order to make a distinction between these two possibilities, the ICD of ANCD was recorded in the presence of 1-adamantylammonium chloride (ADAC). ADAC has a high affinity for encapsulation in β-CD ($K_a=1.1\times10^5$ M^{-1}).[2d] In the case for which the AN residue is inside the β-CD cavity, ADAC is expected to displace it to the outside, leading to a reversal in the sign of the ICD signal. If the AN residue is residing outside the cavity, encapsulation of ADAC is not expected to affect its orientation. When ADAC was added to ANCD solution, the positive ICD spectrum shown in Figure 2B was obtained. ADAC has no absorption in this region and hence is not expected to contribute to the ICD signal. We propose that ANCD exists in a conformation in which the AN moiety is partially encapsulated in β-CD with the long axis

 © 2007 Wiley-VCH Verlag GmbH & Co. KGaA, Weinheim

nearly parallel to the β-CD axis (angle between the two axes $<54.7°$) and when ADAC is added, it is displaced to the outside of the smaller rim.

The singlet excited-state properties of ANCD relevant to our study were obtained from absorption and fluorescence (steady-state and time-resolved) measurements. The results are provided in Table 1. In order to obtain the triplet-state

Table 1. Relevant photophysical and electrochemical parameters of ANCD.

Parameter	Symbol	Value
singlet energy	E_S	3.2 eV
fluorescence quantum yield	Φ_F	0.71
fluorescence lifetime	τ_F	6.8 ns
fluorescence decay constant	k_F	$1.04\times10^8\ s^{-1}$
rate constant for intersystem crossing	k_{ST}	$2.9\times10^7\ s^{-1}$
triplet energy[10]	E_T	1.85 eV
triplet quantum yield	Φ_T	0.21
triplet decay constant	k_T	$2.1\times10^4\ s^{-1}$
oxidation potential[11]	E_{ox}	1.14 V (vs SCE)

properties, laser flash photolysis experiments were carried out. The transient spectrum of ANCD in water (see the Supporting Information Scheme S4) was very similar to the transient spectrum of AN in acetonitrile, and exhibited an absorption maximum at 420 nm and decayed with a lifetime of 47 μs. The transient was quenched by oxygen and we assign the spectrum to the triplet of AN. Relevant parameters obtained from flash photolysis are also summarized in Table 1. The triplet-state energy of ANCD is assumed to be same as that of AN, and the value taken from the literature[10] is given in Table 1. Notice that $\Phi_F+\Phi_T<1$, indicating a small percentage of non-radiative processes taking place in ANCD. This aspect is neglected in subsequent discussions. As the AN residue acts as donor in the PET reaction (see below), the oxidation potential (E_{ox}) of this moiety is an important parameter. Attempts were made to record the cyclic voltammogram of ANCD, but a good oxidation peak could not be obtained. Hence, the E_{ox} of ANCD is assumed to be same as that of 9-alkylanthracene, and a value taken from the literature[11] is given in Table 1.

Electron acceptor: The electron acceptor we employed in this study is a PMDI derivative. The use of PMDI derivatives as electron acceptors in PET reactions is well documented in the literature.[12] The solubility of PMDI in water is very poor. We attached a pyridinium group to one of its nitrogen atoms to make the water-soluble derivative pyromellitic *N*-(2-propyl)-*N*′-(*N*-pyridinium)ethyl diimide (termed PMDI) for use in this study (see the Supporting Information Scheme S5 for synthetic scheme and structure).

PMDI was found to interact with native β-CD in aqueous solution. Addition of β-CD to an aqueous solution of PMDI (1×10^{-4} M) results in a blue shift of the absorption maximum along with slight enhancement in the absorbance (see Figure 3a). A clear isosbestic point was also observed. If a 1:1

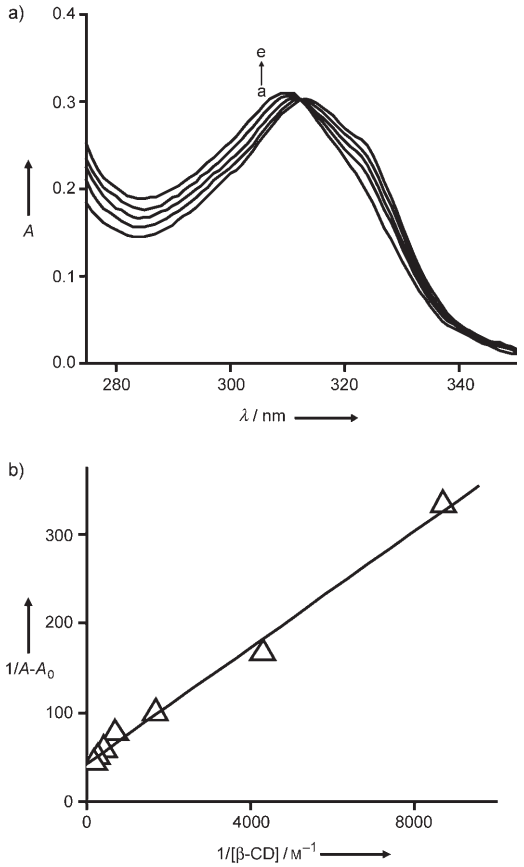

Figure 3. a) Absorption spectra of PMDI (1×10^{-4} M) in the presence of various concentrations of β-CD (1.14×10^{-4}–5×10^{-3} M). b) Plot of $1/(A-A_0)$ against 1/[β-CD].

complex is formed between PMDI and β-CD, a plot of $1/(A-A_0)$ against 1/[β-CD] will be a straight line.[13] The double reciprocal plot was a straight line (Figure 3b) and gave $K_a=1288\ M^{-1}$.

Interaction of ANCD with PMDI: self-assembly and characterization of dyad: Upon mixing aqueous solutions of ANCD and PMDI, the β-CD-based supramolecular dyad (designated as PMDI⊃ANCD) is formed spontaneously. The self-assembly process was studied by using ICD, ^{1}H NMR, CV and fluorescence techniques. The self-assembly process could not be studied by absorption spectroscopy because the absorption due to AN masks the PMDI absorption. Compared to β-CD, the solubility of ANCD is very poor in water and this imposed some constraints in determining the association constant.

An aqueous solution of PMDI did not exhibit circular dichroism. ANCD exhibited a weak negative ICD signal in aqueous solution (Figure 2). When PMDI is added to a solution of ANCD, the weak negative signal due to ANCD is replaced by a strong positive ICD signal with a maximum at 312 nm (Figure 4). The ICD maximum corresponds to PMDI absorption and this clearly indicates that PMDI is associated with the β-CD part of ANCD. The lowest-energy

 © 2007 Wiley-VCH Verlag GmbH & Co. KGaA, Weinheim

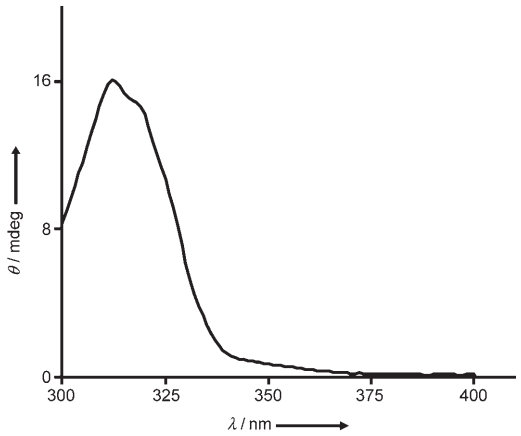

Figure 4. ICD spectrum of a mixture of ANCD (1.3×10^{-4} M) and PMDI (3×10^{-4} M).

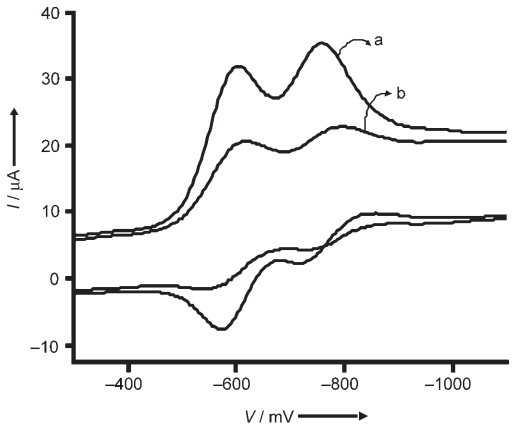

Figure 5. Square-wave voltammogram of PMDI (1.3×10^{-3} M) in the absence (a) and presence (b) of ANCD (1.3×10^{-3} M).

absorption (314 nm) in PMDI derivatives is known to be polarized along the long axis connecting the two imide nitrogen atoms.[14] As per the ICD rules described earlier, the strong positive signal indicates that PMDI enters the β-CD cavity with its long axis parallel to the β-CD axis, with the isopropyl group inside the cavity and the pyridinium moiety projecting out into the aqueous environment. A parallel orientation in which the pyridinium moiety remains inside and the isopropyl group remains outside is ruled out, based on the hydrophilicity/hydrophobicity properties of these groups. When PMDI enters the cavity, the AN residue, which is partially included within the cavity, has to be displaced. A weak positive ICD signal can result at $\lambda > 350$ nm if the displaced AN remains just outside the β-CD cavity. The signal above 350 nm is very weak and does not give any information about the conformation of the displaced AN moiety.

A positive ICD signal from PMDI may also arise if it remains outside the cavity with its long axis perpendicular to the β-CD axis. We have discarded this conformation for the following reasons. If PMDI lies on a rim, it can do so only at the larger rim because the smaller rim is crowded due to the presence of an AN residue. The ICD signal intensity will be very low in this case (rule 3). In such a conformation, the absorption polarization is perpendicular to the CD axis, leading to further reduction in the ICD signal intensity (rule 4). The ICD signal obtained is very strong and does not support this conformation. The ICD signal shown in Figure 4 decreases upon addition of ADAC, and this clearly indicates that PMDI is actually included within the cavity.

Further evidence for the encapsulation of PMDI in the cavity of ANCD is obtained from CV studies. The cyclic voltammogram (see the Supporting Information Scheme S6) and square-wave voltammogram (Figure 5) of PMDI consist of two reversible reduction peaks at −0.58 and −0.74 V (versus SCE). Addition of ANCD results in a reduction of the peak current, which is indicative of complex formation between the two species.

Association of an electroactive guest with a bulky host, such as β-CD, always results in substantial reduction of the effective diffusion coefficient, leading to a decrease in the current associated with the redox process.[15] In addition to the decrease in current, addition of ANCD also results in a slight shift (0.04 V) in the second reduction peak to a more negative $E_{1/2}$ value. A negative shift in the reduction potential indicates destabilization of the reduced state (or reduction has become more difficult). It has been suggested that the redox process in an included guest will occur only after the dissociation of the inclusion complex,[16] leading to a positive shift in the oxidation potential and a negative shift in the reduction potential. These results suggest that PMDI is included in the cavity of ANCD with one of its imide groups deeply buried inside the cavity and the other imide group relatively exposed to water and accessible for reduction at the electrode.

Further evidence for the association of PMDI with ANCD is obtained from ^{1}H NMR spectroscopic studies (see Figure 6). The ^{1}H NMR spectrum of PMDI in D_2O is shown in the lower panel, and the assignments of the different signals are also indicated (the large peak around $\delta = 4.8$ ppm is due to HOD present in D_2O). Upon addition of ANCD, noticeable changes are observed in the chemical shifts of several protons. The CH_3 protons of the isopropyl group (labelled a) appeared as a doublet at $\delta = 1.47$ ppm. Upon addition of ANCD, the doublet changes into a broad singlet and shifts upfield. The CH proton of the isopropyl group (labelled b), which originally was a multiplet, shifted upfield and changed into a broad singlet. The CH_2 group attached to the imide nitrogen (labelled d) also showed similar changes. The most observable change, however, is that of the aromatic pyromellitic imide proton (labelled c). This proton underwent an upfield shift of about 0.4 ppm. The protons in the pyridinium ring (f, g and h) did not exhibit any change, and any change in the e signal is obscured by the β-CD protons of ANCD. The new peaks that appear in the aromatic region are due to the AN moiety of ANCD. In Figure 7 we have plotted the changes observed in the chemical shifts ($\Delta\delta$) for the various protons. It can be seen that even at the highest possible concentration of ANCD, the $\Delta\delta$ values have not

 © 2007 Wiley-VCH Verlag GmbH & Co. KGaA, Weinheim

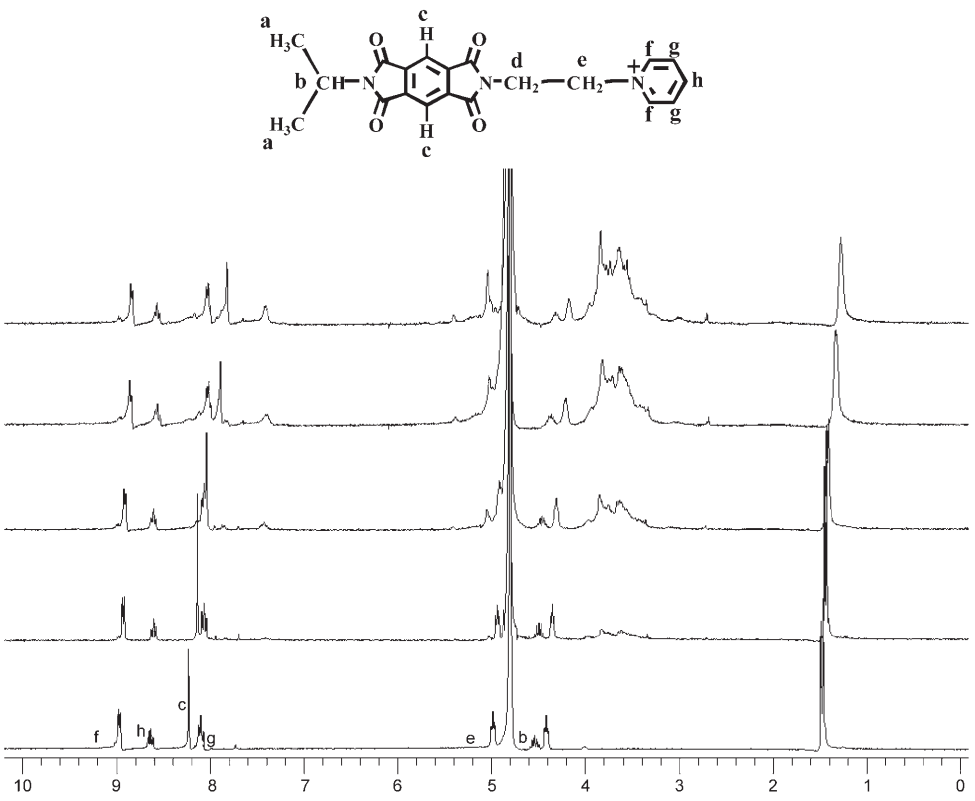

Figure 6. ^{1}H NMR spectra of PMDI in D_2O in the presence of an increasing concentration of ANCD.

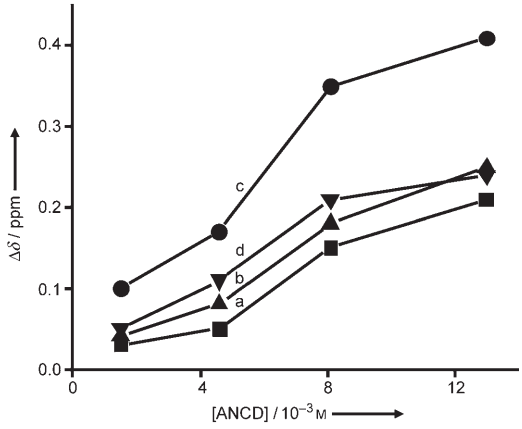

Figure 7. Plot of $\Delta\delta$ against ANCD concentration.

reached a plateau region. Hence, a K_a value could not be determined from the data in Figure 7.

The dimensions of the β-CD cavity taken from the literature[2b] and the molecular dimensions of PMDI obtained from AM1 calculations,[17] along with results from the ICD, CV and ^{1}H NMR studies were put together to obtain a clear picture of the structure of the inclusion complex PMDI⊃ANCD. Relevant molecular dimensions and a possible structure of the inclusion complex are shown in Scheme 2. As the smaller rim of ANCD is capped by AN, PMDI may enter the cavity through the wider rim with the hydrophobic *N*-(2-propyl) end going into the cavity and the hydrophilic *N*′-(2-ethylpyridinium) end remaining outside at the wider rim, as shown in Scheme 2. The ^{1}H NMR signals for the a and b protons have broadened considerably, indicating that free rotation of the 2-propyl group is constrained. The distance between the farthest hydrogen atoms in the 2-propyl group (obtained from AM1) is 4.32 Å. The diameter of the smaller rim of the β-CD cavity is 5.6 Å. The AN moiety and six CH_2OH groups are also present at the smaller rim and hindrance to free rotation of the 2-propyl group is interpreted to mean that this group is situated very close to the narrow rim and flanged by the overhanging CH_2OH and AN residues. The c proton experiences the maximum shift, which indicates that this proton is near the centre of the β-CD cavity. The d-proton signal is also affected and we suggest that this group is present near the wider rim of ANCD. The protons in the pyridinium ring (f, g and h) are unaffected and it can be safely assumed that the pyridinium ring is present outside the cavity fully exposed to water. All of these assignments are consistent with the conformation shown in Scheme 2. The imide group at the pyridinium end is near the wider rim slightly exposed to water and the imide group at the 2-propyl end is buried inside the cavity, supporting the results from CV studies.

As the diameter of the smaller rim of the β-CD cavity is only 5.6 Å, encapsulation of PMDI in this fashion would lead to the displacement of the AN residue, as shown in Scheme 2. The edge-to-edge distance between the PMDI

 © 2007 Wiley-VCH Verlag GmbH & Co. KGaA, Weinheim

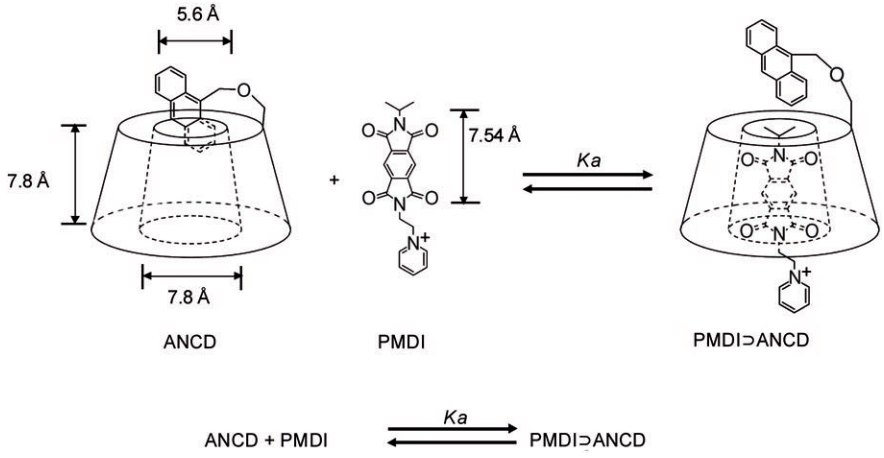

Scheme 2. Inclusion of PMDI into ANCD. Molecular dimensions are also shown.

and AN residues is an important parameter in the electron-transfer process and we assume that this distance is very small (< 2 Å).

PET between β-CD-appended AN and PMDI: When aqueous solutions of ANCD and PMDI are mixed, a fraction of the molecules exist as PMDI⊃ANCD (see Scheme 2). Photoexcitation of the system would then lead to unimolecular and bimolecular electron-transfer processes, as demonstrated previously for α-CD-appended systems[4] and hydrogen-bonded systems.[18] An important difference in the present study is that the triplet excited state of the AN chromophore is also involved in the electron-transfer process.

Fluorescence-quenching experiments: As shown in Figure 8, the fluorescence of ANCD is quenched very efficiently by millimolar concentrations of PMDI. The fluorescence quenching is attributed to electron transfer from the singlet excited state of AN to PMDI, as shown in Equation (1).

$$^1\text{ANCD} \xrightarrow{\text{PMDI}} {}^{\cdot+}\text{ANCD} + \text{PMDI}^{\cdot-} \quad (1)$$

As the singlet energy of PMDI is greater than the singlet energy of AN, quenching by the energy-transfer mechanism is ruled out. The change in free energy associated with this electron-transfer process can be calculated by using the Weller equation [Eq. (2)].[19]

$$\Delta G^0_{(S)} = E_{ox} - E_{red} - E_S - e^2/\varepsilon d \quad (2)$$

in which E_{ox} is the oxidation potential of AN, E_{red} is the first reduction potential of PMDI, E_S is the singlet energy of AN, ε is the dielectric constant of water and d is the distance separating the donor and acceptor. Since ε for water is very high, the last term can be neglected in the calculation. Substitution of the various values gave $\Delta G^0_{(S)} = -1.48$ eV. The highly negative $\Delta G^0_{(S)}$ value suggests that the singlet-state-mediated electron-transfer process lies in the Marcus inverted region.[20]

The singlet-state quenching process can occur by a unimolecular mechanism (intramolecular quenching within PMDI⊃ANCD), a diffusion-mediated mechanism or a combination of these mechanisms. For CD-appended systems, the diffusion coefficient (k_{diff}) in water is determined to be $6.6\times10^9\,\text{M}^{-1}\text{s}^{-1}$.[3c] If the quenching occurred by the diffusion mechanism, the maximum possible rate constant $k_q = k_{diff}$. By definition, $k_q\tau_0 = K_{SV}$, in which K_{SV} is the Stern–Volmer constant.

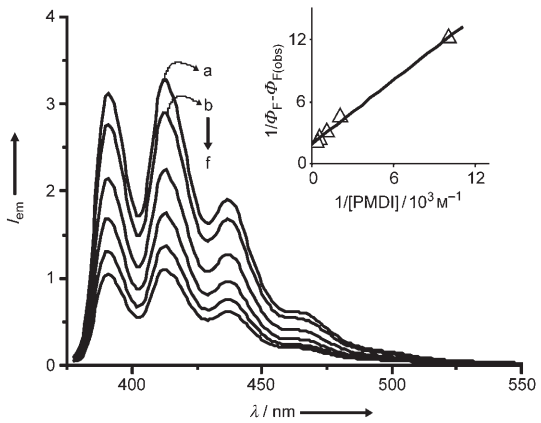

Figure 8. Quenching of ANCD fluorescence by increasing concentrations of PMDI (1×10^{-4}–3×10^{-3} M).

Substituting k_{diff} and τ_0, we obtain $K_{SV} = 45\,\text{M}^{-1}$. By definition, the reciprocal of K_{SV} gives the concentration (of the quencher) required to quench 50% of the fluorescence.[21] This calculation revealed that 2.2×10^{-2} M PMDI is required for 50% quenching if quenching is to occur by the diffusion mechanism. Figure 8 shows that nearly 75% of the fluorescence is quenched by 3.0×10^{-3} M PMDI. We propose that in the concentrations employed for the fluorescence quenching experiments, the diffusion-mediated reaction does not contribute significantly to singlet-state deactivation.

In the absence of diffusion-mediated quenching, the observed fluorescence quantum yield ($\Phi_{F(obs)}$) can be related to the fluorescence quantum yields of the uncomplexed (Φ_F) and complexed ($\Phi_{F(PMDI\supset ANCD)}$) forms by Equation (3)].[22]

$$\Phi_{F(obs)} = (1-\alpha)\Phi_F + \alpha\Phi_{F(PMDI\supset ANCD)} \quad (3)$$

in which α is the fraction of associated molecules. Equation (3) could be simplified to [Eq. (4)].

 © 2007 Wiley-VCH Verlag GmbH & Co. KGaA, Weinheim

$$\frac{1}{\Phi_F-\Phi_{F(obs)}}=\frac{1}{\Phi_F-\Phi_{F(PMDI\supset ANCD)}}+\frac{1}{K_a(\Phi_F-\Phi_{F(PMDI\supset ANCD)})[PMDI]} \quad (4)$$

The linear dependence between $1/(\Phi_F-\Phi_{F(obs)})$ and $1/[PMDI]$ (inset in Figure 8) supports this mechanism. The association constant K_a and the fluorescence quantum yield of the complex ($\Phi_{F(PMDI\supset ANCD)}$) could be obtained from the intercept and slope of this plot. This analysis gave $K_a=1800\ M^{-1}$ and $\Phi_{F(PMDI\supset ANCD)}=0.214$. The rate constant for electron transfer ($k_{et(S)}$) within PMDI⊃ANCD can be obtained by using Equation (5). Substituting the values, we obtain $k_{et(S)}=3.4\times10^8\ s^{-1}$.

$$k_{et(S)}=\frac{1}{\tau_F}\left(\frac{\Phi_F}{\Phi_{F(PMDI\supset ANCD)}}-1\right) \quad (5)$$

Further insight into the mechanism of fluorescence quenching is obtained by fluorescence lifetime experiments. In the absence of any quencher, the fluorescence decay of ANCD was monoexponential. The decays become biexponential (Figure 9) in the presence of PMDI.

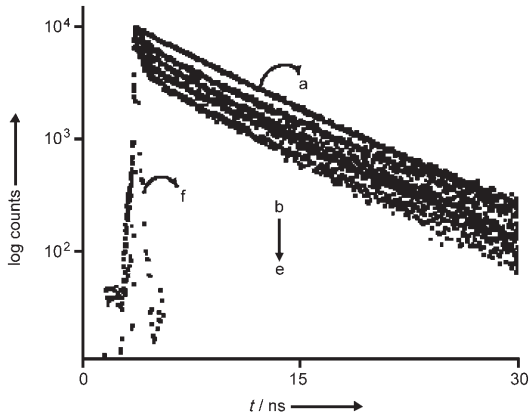

Figure 9. Fluorescence decay profiles of ANCD in the absence (a) and presence (b–e) of different concentrations ($1–8\times10^{-4}$ M) of PMDI. f) is the lamp profile.

All the fluorescence decay profiles were fitted by using the biexponential function [Eq. (6)].

$$I_t=\chi_{(PMDI\supset ANCD)}\exp(-t/\tau_1)+\chi_{(ANCD)}\exp(-t/\tau_2) \quad (6)$$

in which $\chi_{(PMDI\supset ANCD)}$ is the mole fraction of the complexed species and $\chi_{(ANCD)}$ is the mole fraction of free ANCD. Values of τ_1, τ_2, $\chi_{(PMDI\supset ANCD)}$ and $\chi_{(ANCD)}$ along with χ^2 values obtained from the fit are given in Table 2.

The short lifetime component arises due to electron-transfer quenching within the ensemble PMDI⊃ANCD and hence $\tau_1=(k_0+k_{et(S)})^{-1}$, in which $k_{et(S)}$ is the rate constant for electron transfer within PMDI⊃ANCD. $k_{et(S)}$ can be calculated by using Equation (7)].[4]

Table 2. Fluorescence lifetimes (τ_1 and τ_2), fractional contributions ($\chi_{(PMDI\supset ANCD)}$ and $\chi_{(ANCD)}$) and χ^2 values obtained for fluorescence lifetime quenching of ANCD by PMDI.

[PMDI] ($\times10^{-4}$ M)	τ_1 [ns]	$\chi_{(PMDI\supset ANCD)}$	τ_2 [ns]	$\chi_{(ANCD)}$	χ^2
0	–	–	6.8	100	1.2
1	2.4	8.36	6.8	91.64	1.1
2	2.5	13.09	6.7	86.91	1.1
3	2.5	16.06	6.7	83.94	1.2
5	2.5	38.91	6.7	61.09	1.1
8	2.6	49.98	6.6	50.02	1.1

$$k_{et(S)}=1/\tau_1-1/\tau_0 \quad (7)$$

The value of k_{et} thus obtained was $2.5\times10^8\ s^{-1}$. The $k_{et(S)}$ value calculated from steady-state quenching (see above) is very close to this value. It can be noticed from Table 2 that the long lifetime component $\tau_2\approx\tau_0$, which indicates that the contribution due to diffusion-mediated quenching of the singlet excited state is negligible.

K_a for the encapsulation process can be calculated by using $\chi_{(PMDI\supset ANCD)}$ and $\chi_{(ANCD)}$.[4] As the concentration of PMDI is large compared to that of the complex, we can write [Eq. (8)].

$$K_a=\frac{\chi_{(PMDI\supset ANCD)}}{\chi_{(ANCD)}[PMDI]} \quad (8)$$

A plot of $\chi_{(PMDI\supset ANCD)}/\chi_{(ANCD)}$ against [PMDI] was linear (see the Supporting Information Scheme S7) and gave $K_a=1390\ M^{-1}$. This value is comparable to the K_a value calculated by using UV/visible spectroscopy and somewhat smaller than the value obtained from the steady-state fluorescence method (see above).

Electron transfer within PMDI⊃ANCD is an example of non-adiabatic electron transfer involving a weakly interacting donor and acceptor for which the rate constant can be obtained by using the modified Marcus equation [Eq. (9)].[23]

$$k_{et}=(2\pi/\hbar)H_{el}^2(4\pi\lambda_0k_BT)^{-1/2}\sum_{m=0}^{\infty}(e^{-s}s^m/m!)\times\exp[-(\lambda_0+\Delta G^0+mh\nu)^2/(4\lambda_0k_BT)] \quad (9)$$

in which $\hbar$ is Planck's constant divided by 2π, H_{el} is the coupling matrix element, λ_o is the outer-sphere reorganization energy, k_B is the Boltzmann constant, T is the absolute temperature, ΔG^0 is the change in free energy for the reaction, $s=\lambda_i/h\nu$, m is an integer, and λ_i is the inner-sphere reorganization energy. In our earlier study[4] with α-CD-appended pyrene and encapsulated acceptors, we obtained $H_{el}=3\ cm^{-1}$. By using $H_{el}=3\ cm^{-1}$, $\lambda_0=0.8$ eV, $\lambda_i=0.2$ eV, $h\nu=0.15$ eV, $T=298$ K and $\Delta G^0=-1.48$ eV, we obtain $k_{et(S)}=3.83\times10^8\ s^{-1}$. Notice that this value is very close to the values obtained from steady-state ($3.4\times10^8\ s^{-1}$) and time-resolved ($2.5\times10^8\ s^{-1}$) fluorescence-quenching measurements.

 © 2007 Wiley-VCH Verlag GmbH & Co. KGaA, Weinheim

Laser flash photolysis: Laser flash photolysis of ANCD resulted in the formation of the AN triplet state absorbing at 420 nm (Supporting Information Scheme S4). We observed that the triplet is quenched by PMDI. The quenching rate constant ($k_{q(T)} = 1.6 \times 10^8\ M^{-1} s^{-1}$) was obtained by plotting the observed pseudo-first-order rate constants against [PMDI] (see the Supporting Information Scheme S8). The triplet energy of PMDI (2.45 eV) is ≈ 0.6 eV higher than the triplet energy of AN.[24] Hence, quenching by an energy-transfer mechanism is ruled out. Based on the evidence obtained from flash photolysis experiments, we attribute the quenching to an electron-transfer process that takes place from the triplet state of AN [Eq. (10)]:

$$^3\text{ANCD} \xrightarrow{\text{PMDI}} {}^{\bullet+}\text{ANCD} + \text{PMDI}^{\bullet-} \quad (10)$$

The change in free energy for electron transfer from the triplet state ($\Delta G^0_{(T)}$) can also be calculated from Equation (2), by substituting the triplet energy E_T instead of E_S. We obtained $\Delta G^0_{(T)} = -0.12$ eV. The $k_{q(T)}$ value obtained is much lower than the diffusion limit, probably because of the low driving force for this reaction. As mentioned previously, ^{3}ANCD was quenched by oxygen. In order to make a comparison, the rate constant for oxygen quenching ($k_q(O_2)$) was determined and the value obtained was $9.0 \times 10^8\ M^{-1} s^{-1}$, indicating that quenching of ^{3}ANCD by oxygen is five times more efficient than quenching by PMDI.

PMDI has no absorption above 350 nm and hence AN can be selectively excited in the presence of PMDI by using the 355 nm laser light. The photoprocesses taking place in the system are expected to depend on the position of the equilibrium shown in Scheme 2. At lower concentrations of PMDI, the equilibrium is in favour of intermolecular reactions (involving ^{3}ANCD), and at higher concentrations of PMDI intraensemble processes (singlet-state-mediated reactions within PMDI⊃ANCD) dominate. In order to understand these processes in detail, transient absorption spectra of ANCD were recorded at several different concentrations of PMDI. Figure 10a and b show the transient absorption spectra taken at $[PMDI] = 7 \times 10^{-5}$ and 5×10^{-3} M, respectively. In both cases the spectra exhibited maxima at 420 and 720 nm. The 720 nm absorption is due to $PMDI^{\bullet-}$ and $AN^{\bullet+}$,[25,26] and the 420 nm absorption is due to ^{3}ANCD and $AN^{\bullet+}$. At low [PMDI], the 420 nm band due to ^{3}ANCD is very strong (Figure 10a). Kinetic traces taken in a small time window show decay of the triplet at 420 nm and a matching growth of the radical-ion products at 720 nm (see insets in Figure 10a), confirming that the products originate through the triplet pathway shown in Equation (10).

The quantum yield (Φ_{cs}) for the formation of the CS state was estimated (see Experimental Section) by assuming that the absorption at 720 nm is due to equimolar amounts of $PMDI^{\bullet-}$ and $AN^{\bullet+}$. Φ_{cs} was found to increase with [PMDI] and reach a maximum at $[PMDI] = 5 \times 10^{-3}$ M (see the Supporting Information Scheme S9). This result suggests that the yield of the radical-ion products increases with an increase in the fraction of the PMDI⊃ANCD complex. In the transient spectrum taken at $[PMDI] = 5 \times 10^{-3}$ M (Figure 10b), the 720 nm band is much stronger than the 420 nm

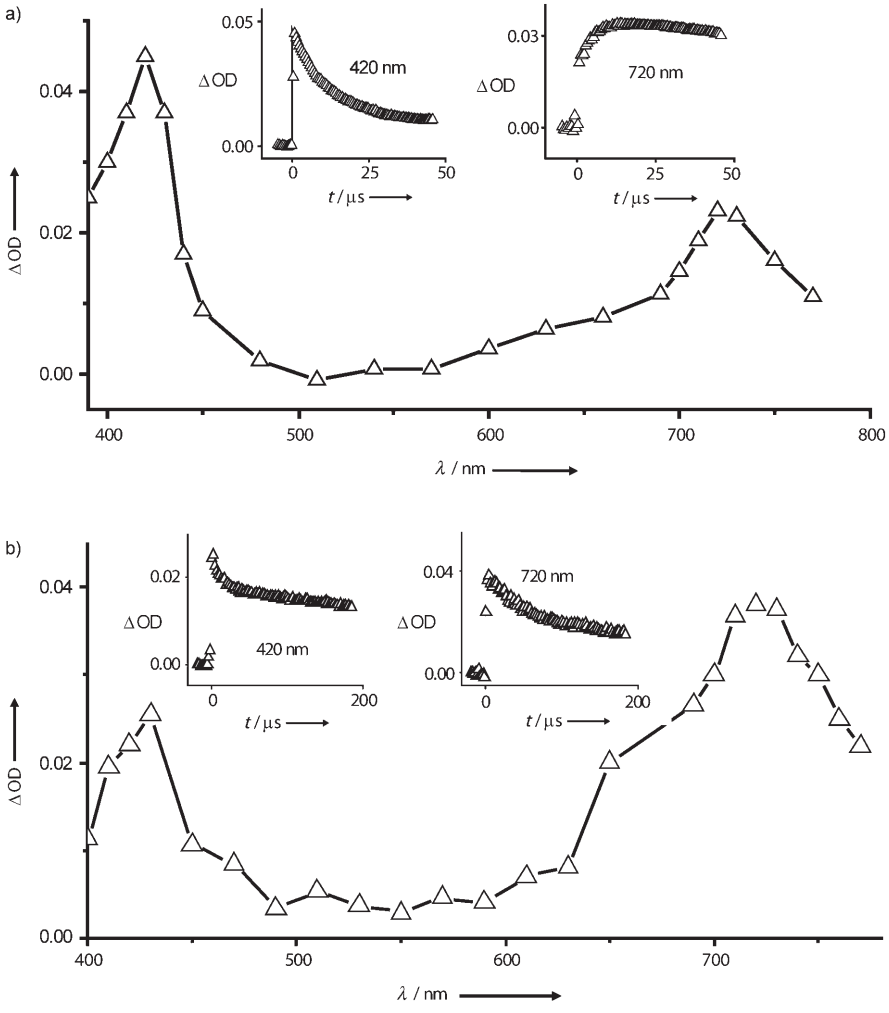

Figure 10. Transient absorption spectrum of ANCD (7×10^{-5} M) in the presence of a) 7×10^{-5} M PMDI recorded at 0.46 μs and b) 5×10^{-3} M PMDI recorded at 1.0 μs following the laser flash. Insets show the decays at 420 and 720 nm.

© 2007 Wiley-VCH Verlag GmbH & Co. KGaA, Weinheim

band, indicating that the contribution from the triplet state is small. At 420 nm, the decay exhibited a fast component due to decay of ^{3}AN and a very slow component due to decay of AN$^{\bullet+}$ (see inset in Figure 10b). Notice that the absorption due to the radical-ion products at 720 nm is very long-lived and persists even after 200 μs.

Results from the fluorescence quenching and flash photolysis experiments can be summarized as shown in Equations (11–16) to describe the various intra-ensemble processes taking place in the system. Complex formation will not affect the fundamental photophysical rate constants k_F, k_{ST} and k_T. Complex formation, however, leads to electron-transfer processes from singlet as well as triplet states characterized by rate constants $k_{et(S)}$ and $k_{et(T)}$. The $k_{et(S)}$ value obtained from lifetime experiments is given in Equations (11–16). The rate constant for electron transfer from the triplet state within the ensemble ($k_{et(T)}$) could not be determined experimentally. This value was calculated by using Equation (9) and by employing the same parameters described earlier along with $\Delta G^0_T = -0.12$ eV. This treatment gave $k_{et(T)} = 2.22\times10^5\ s^{-1}$ and this value is shown in Equations (11–16).

$$\text{PMDI}\supset\text{ANCD}\xrightarrow{h\nu}\text{PMDI}\supset{}^1\text{AN*CD} \quad (11)$$

$$\text{PMDI}\supset{}^1\text{AN*CD}\xrightarrow[1.04\times10^8\ s^{-1}]{k_F}\text{PMDI}\supset\text{ANCD} \quad (12)$$

$$\text{PMDI}\supset{}^1\text{AN*CD}\xrightarrow[2.5\times10^8\ s^{-1}]{k_{et(S)}}{}^{-\bullet}\text{PMDI}\supset\text{AN}^{+\bullet}\text{CD} \quad (13)$$

$$\text{PMDI}\supset{}^1\text{AN*CD}\xrightarrow[2.9\times10^7\ s^{-1}]{k_{ST}}\text{PMDI}\supset{}^3\text{AN*CD} \quad (14)$$

$$\text{PMDI}\supset{}^3\text{AN*CD}\xrightarrow[2.1\times10^4\ s^{-1}]{k_T}\text{PMDI}\supset\text{ANCD} \quad (15)$$

$$\text{PMDI}\supset{}^3\text{AN*CD}\xrightarrow[2.2\times10^5\ s^{-1}]{k_{et(T)}}{}^{-\bullet}\text{PMDI}\supset\text{AN}^{+\bullet}\text{CD} \quad (16)$$

The quantum yield of the various intra-ensemble processes can be obtained by using the k values. For example, $\Phi_{et(S)} = k_{et(S)}/(k_{et(S)}+k_F+k_{ST})$ and so on. The values so obtained are: $\Phi_{et(S)}$(complex) = 0.65, Φ_T(complex) = 0.076 and $\Phi_{et(T)}$(complex) = 0.069. Thus, 71.9% of the excited AN in the PMDI⊃ANCD complex decays by electron-transfer processes. According to the arguments we have presented, at [PMDI] = 5×10^{-3} M, ANCD is present mostly as the complex PMDI⊃ANCD and within the complex more than 70% of excited AN decays by electron-transfer processes. The value of Φ_{cs}, however, is only 0.105 under these conditions (Supporting Information Scheme S9). This suggests that a significant fraction of the radical ions formed underwent back electron transfer (BET) before they could be detected.

An important observation here is that a fraction of the CS state survives for more than 200 μs. Generation of a long-lived CS state is an important aim in the study of PET reactions.[27] Long-lived decay, as shown in Figure 10b, is generally associated with intermolecular processes. Covalently bound donor–acceptor dyads in general (with the exception of C_{60}-based systems) exhibit very short lifetimes, although a claim to the contrary has been made recently.[28] For a few CD-based dyads for which data are available, the CS-state lifetimes were extremely small.[3m–q] In this context it was important to know if the long-lived CS state (shown in insets of Figure 10b) has any contribution from the intra-ensemble electron-transfer processes. Laser flash photolysis in oxygen-saturated solutions suggested that a fraction of the long-lived CS state actually originated through the intra-ensemble pathway.

The concentration of oxygen in oxygen-saturated aqueous solutions is 1.39×10^{-3} M.[29] We have already shown that for ^{3}ANCD, k_q for oxygen is five times larger than k_q for PMDI. Under conditions in which [O_2] > [PMDI], quenching of ^{3}ANCD by PMDI is not expected to be efficient. Laser flash photolysis of the system under the conditions described for Figure 10a was carried out after saturating the solution with oxygen. Under these conditions the only transient observed was a fast-decaying triplet. It should be mentioned that in addition to triplets, oxygen also quenches radical anions very efficiently, but radical cations are generally not quenched. The presence of oxygen is not expected to affect the intra-ensemble processes. As the absorption due to AN$^{\bullet+}$ at 720 nm was absent, we conclude that under the conditions used for Figure 10a, only intermolecular electron-transfer quenching was possible, and this process was inhibited completely by the oxygen present in the solution.

We carried out oxygen-quenching experiments at [PMDI] = 1.0×10^{-3} M. If we assume that $K_a = 10^3\ M^{-1}$ and $[\text{PMDI}]_{eq} \approx [\text{PMDI}]_0$ (in which $[\text{PMDI}]_0$ is the actual concentration and $[\text{PMDI}]_{eq}$ is the equilibrium concentration of PMDI), it can be shown that [PMDI⊃ANCD]/[ANCD] = 1 under these conditions. Fifty per cent of ANCD is present in the free form and undergoes triplet-mediated electron transfer and the remaining 50% is present as the complex and undergoes intra-ensemble electron transfer. It can be shown that nearly 78% of all the PET reactions occur within the ensemble and the remaining 22% occur through the intermolecular triplet pathway. Saturating the solution with oxygen is expected to remove most of the intermolecular electron transfers and any radical ions observed under these conditions could be considered as arising from the intra-ensemble pathway.

Figure 11 shows the kinetic traces at 420 and 720 nm for the oxygen-saturated ANCD (7×10^{-5} M) solution in the presence of 1×10^{-3} M PMDI. At 420 nm, the initial fast decay is due to the triplet and the long-lived residual absorption is due to AN$^{\bullet+}$. At 720 nm, the fast decay is assigned to oxygen quenching of PMDI$^{\bullet-}$ and the residual absorption is due to AN$^{\bullet+}$. By using the residual absorption, Φ_{cs} was calculated and the value obtained was 0.056. In the absence of oxygen, Φ_{cs} was 0.08. This study prompted us to suggest that more than 50% of the CS state observed under argon-saturated conditions originated from the intra-ensemble pathway at high PMDI concentrations.

The reason for the long lifetime of the CS state is not exactly understood. The following factors, however, can contribute. 1) A small fraction of the radical-ion products arise through the triplet pathway [Eq. (16)]. BET in the triplet ion pair is spin forbidden and hence slow. 2) AN and PMDI

 © 2007 Wiley-VCH Verlag GmbH & Co. KGaA, Weinheim

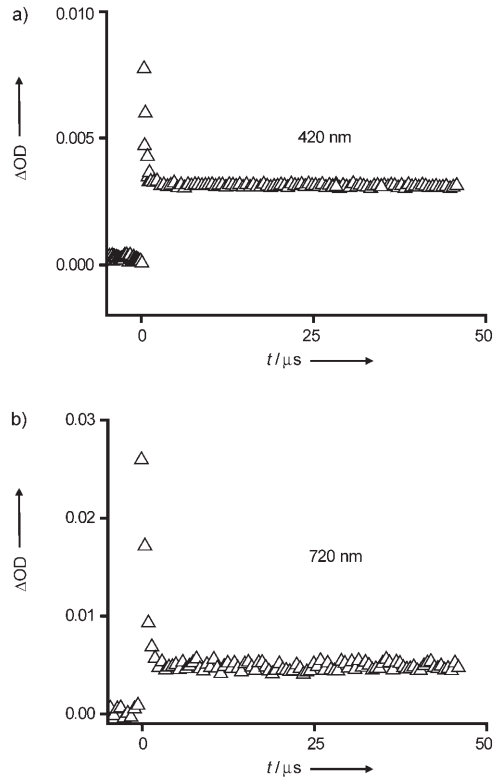

Figure 11. Kinetic traces at 420 (a) and 720 nm (b) for the oxygen-saturated ANCD (7×10^{-5} M) solution in the presence of 1×10^{-3} M PMDI.

units in PMDI⊃ANCD are separated by a small distance and if there are no water molecules in this space, the BET has to occur either through space or through several bonds of the β-CD framework, leading to low BET rates. 3) The $PMDI^{\bullet-}$ formed is polar and may exhibit a tendency to move out to the polar aqueous environment, leading to an increase in distance between $AN^{\bullet+}$ and $PMDI^{\bullet-}$. Control of BET by this latter mechanism has been suggested in a few cases.[30] 4) For the AN–PMDI system studied here, $\Delta G^0_{(BET)}=-1.72$ and $\lambda\approx1$ eV. Thus, the BET process occurs in the deep inverted region and this can also result in an enhanced lifetime for the CS state. Fukuzumi and co-workers have recently observed a long lifetime for the CS state in a π complex formed between co-facial free-base bisporphyrin and the acridinium ion.[31] The long lifetime of the CS state was attributed to inverted region effects in this case.

Conclusion

We have assembled a supramolecular dyad PMDI⊃ANCD with the AN donor covalently attached to β-CD and a PMDI acceptor encapsulated within the β-CD cavity. The encapsulation process was studied by UV/Vis, ICD, ^{1}H NMR, CV and fluorescence techniques. The association constant was determined by three methods. The results suggested that the PMDI moiety is encapsulated with the aromatic ring at the centre of the cavity. The *N*-(2-propyl) end of PMDI is at the narrower rim and the *N*-ethylpyridinium end is at the wider rim exposed to the aqueous medium. PMDI quenches the singlet and triplet excited states of AN by an electron-transfer mechanism. The radical cation of AN and radical anion of PMDI were observed in flash photolysis experiments. At $[PMDI]<10^{-4}$ M, the system exists as free molecules and fluorescence quenching is negligible. AN radical cations and PMDI radical anions are formed even under these conditions, and this is attributed to diffusion-mediated triplet quenching. At higher concentrations of PMDI, the equilibrium is largely in favour of PMDI⊃ANCD and intra-ensemble PET processes taking place. The rate constant for electron transfer within the ensemble from the singlet excited state of AN was measured. The experimentally determined rate constant agreed very well with that calculated using the Marcus equation. A fraction of the CS state was very long lived, suggesting that the non-covalent approach is useful in the design of artificial photosynthetic systems.

Experimental Section

Materials: ANCD was prepared as shown in Scheme 1. 9-Bromomethylanthracene (0.4 g) was added to a solution of β-CD (1.7 g, 1.49 mmol) in 2,6-lutidine (40 mL) and dry DMF (40 mL) and the mixture was heated at 150 °C under an argon atmosphere for 3.5 h. The solvents were removed under vacuum and the solid was washed several times with ethyl acetate and purified by chromatography over silica gel by using methanol/ethyl acetate 1:1 as the eluent. The product was further purified by chromatography (Sephadex column) by using deionized water as the eluent. The yield of purified product was 25%. ^{1}H NMR (300 MHz, [D$_6$]DMSO, 25 °C, TMS): $\delta=7.8$–8.6 (m, 9H), 5.4–5.9 (m, 14H), 4.4–4.8 (m, 15H), 3.1–3.6 ppm (m, 42H); ^{13}C NMR (75 MHz, [D$_6$]DMSO): $\delta=$ 59.98, 60.31, 64.65, 68.85, 70.73, 71.80, 72.09, 72.48, 73.12, 73.52, 81.57, 82.05, 102.34, 102.58, 124.86, 125.22, 126.48, 126.74, 127.7, 127.93, 128.77, 129.40, 130.47, 130.99 ppm; IR (KBr): $\tilde{\nu}=1031$, 1080, 1153, 1246, 1334, 1365, 1448, 1587, 1662, 2895, 2939 cm^{-1}; UV/Vis (water): λ_{max} (ε) = 368 nm (8500 M^{-1}cm^{-1}); MS (MALDI-TOF): *m*/*z*: 1325 $[M+H]^+$.

PMDI was prepared by adapting a standard procedure[32] (see the Supporting Information Scheme S5 for synthetic scheme and experimental details). ^{1}H NMR (300 MHz, D$_2$O, 25 °C): $\delta=8.96$ (d, 2H), 8.63 (t, 1H), 8.23 (s, 2H), 8.09 (t, 2H), 4.98 (t, 2H), 4.52–4.56 (m, 1H), 4.41 (t, 2H), 1.47 ppm (d, 6H); ^{13}C NMR (75 MHz, [D$_6$]DMSO, 25 °C, TMS): $\delta=$ 19.75, 40.34, 42.99, 59.58, 117.29, 128.09, 136.67, 136.99, 145.47, 146.20, 166.05, 166.10 ppm; IR (KBr): $\tilde{\nu}=3055$, 2985, 1768, 1709, 1631 cm^{-1}; UV/Vis (water): λ_{max} (ε) = 314 nm (2840 M^{-1}cm^{-1}); HRMS: *m*/*z*: 364.02 $[M]^+$.

The 9-chloromethylanthracene used in the study was purchased from Aldrich and converted to AMTAC by adapting standard procedures.[33] 1-Adamantylamine was purchased from Aldrich and converted to ADAC by treatment with aqueous hydrochloric acid. AN and benzophenone (BP) were purchased from Aldrich and recrystallised before use.

Methods: NMR spectra were recorded by using a 300 MHz Bruker Avance DPX spectrometer. MALDI mass spectrometry was conducted on a Perspective Biosystems Voyager DEPRO MALDI-TOF spectrometer in a matrix of α-cyano-4-hydroxycinnamic acid. High-resolution mass spectra were obtained by using a JOEL JMS600 mass spectrometer. Absorption spectra were obtained by using a Shimadzu 3101PC UV/Vis–NIR scanning spectrophotometer. ICD spectra were obtained by using a JASCO J-810 circular dichroism spectropolarimeter. Steady-state fluorescence experiments were performed with a SPEX Fluorolog F112X spectrofluorimeter by using optically dilute solutions. The fluorescence quantum yield of ANCD in water was determined by the relative method em-

 © 2007 Wiley-VCH Verlag GmbH & Co. KGaA, Weinheim

ploying an optically matched solution of AN in ethanol as reference ($\Phi_R = 0.27$).[34] The following equation was used [Eq. (17)].[35]

$$\Phi_F = \Phi_R \frac{A \mathrm{OD}_R n^2}{A_R \mathrm{OD} n_R{}^2} \quad (17)$$

in which the subscript R refers to the reference, OD is the optical density at the excitation wavelength, n is the refractive index of the solvent and A is the area under the fluorescence spectrum. CV experiments were performed by using a BAS 50 W voltammetric analyser. Solutions of the compounds (1×10^{-3} M) in water containing 0.1 M potassium nitrate were thoroughly deaerated and used for CV experiments. Time-resolved fluorescence experiments were performed by using an IBH picosecond single-photon counting system employing a 401 nm nano-LED excitation source and a Hamamatsu C4878-02 microchannel plate (MCP) detector. Laser flash photolysis experiments were performed by using an Applied Photophysics Model LKS-20 laser kinetic spectrometer by using the third harmonic (355 nm) from a GCR-12 series Quanta Ray Nd:YAG laser. Quantum yields of the triplet (Φ_T) and CS (Φ_{CS}) states were determined by relative actinometry employing a solution of BP in benzene as reference. The following equation was used [Eq. (18)].[36]

$$\Phi_M = \Phi_R \frac{\Delta \mathrm{OD}_M \varepsilon_R}{\Delta \mathrm{OD}_R \varepsilon_M} \quad (18)$$

in which the subscript M refers to the state under consideration (triplet or CS state) and R refers to BP; ΔOD is the end-of-pulse optical density of transients and ε the extinction coefficients of transients. For BP, values of $\Phi_R = 1.0$ and $\varepsilon_R = 7600\ \mathrm{M^{-1}cm^{-1}}$ at 530 nm[37] were used. For calculating Φ_T, the reported extinction coefficient of the triplet–triplet absorption of AN ($\varepsilon_T = 45500\ \mathrm{M^{-1}cm^{-1}}$ at 420 nm)[38] was used. For the calculation of Φ_{CS}, known extinction coefficients of the AN radical cation ($\varepsilon_{AN^{\cdot}+} = 11600\ \mathrm{M^{-1}cm^{-1}}$ at 720 nm)[39] and PMDI radical anion ($\varepsilon_{PMDI^{\cdot}-} = 41700\ \mathrm{M^{-1}cm^{-1}}$ at 720 nm)[25] were employed. Rate constants (k) for the various processes were obtained from Φ and τ_F values by using standard equations. Solutions for laser flash photolysis studies were deaerated by purging with argon for 20 min before experiments. Unless stated otherwise, all experiments were performed at 20 °C.

Acknowledgements

This work was supported by the Department of Science and Technology (DST), Government of India, New Delhi, and the Council of Scientific and Industrial Research (CSIR Task Force Programme COR 03), Government of India. B.B. thanks CSIR, Government of India, for a fellowship. This is contribution no. RRLT-PPG-241 from the Photosciences and Photonics section of the Regional Research Laboratory, Trivandrum.

[1] a) J. L. Sessler, B. Wang, S. L. Springer, C. T. Brown in *Comprehensive Supramolecular Chemistry, Vol. 4* (Eds.: J. L. Atwood, J. E. D. Davies, D. D. MacNicol, F. Vögtle, Y. Murakami), Pergamon, Oxford, **1996**, pp. 311–336; b) M. D. Ward, *Chem. Soc. Rev.* **1997**, *26*, 365–375; c) P. Piotrowiak, *Chem. Soc. Rev.* **1999**, *28*, 143–150; d) C. J. Chang, J. D. K. Brown, M. C. Y. Chang, E. A. Baker, D. G. Nocera in *Electron Transfer in Chemistry, Vol. 3* (Ed.: V. Balzani), Wiley-VCH, Weinheim, **2001**, pp. 409–457.

[2] a) A. Ueno, T. Osa in *Photochemistry in Organized and Constrained Media* (Ed.: V. Ramamurthy), Wiley-VCH, New York, **1991**, pp. 739–782; b) J. Szejtli, *Cyclodextrin Technology*, Kluwer Academic, Dordrecht, **1988**; c) *Comprehensive Supramolecular Chemistry, Vol. 3* (Eds.: J. L. Atwood, J. E. D. Davies, D. D. MacNicol, F. Vögtle, J. Szejtli, T. Osa), Pergamon, Oxford, **1996**; d) M. V. Rekharsky, Y. Inoue, *Chem. Rev.* **1998**, *98*, 1875–1918.

[3] a) Y. Kuroda, M. Ito, T. Sera, H. Ogoshi, *J. Am. Chem. Soc.* **1993**, *115*, 7003–7004; b) H. F. M. Nelissen, M. Kercher, L. De Cola, M. C. Feiters, R. J. M. Nolte, *Chem. Eur. J.* **2002**, *8*, 5407–5414; c) Y.-H. Wang, H.-M. Zhang, L. Liu, Z.-X. Liang, Q.-X. Guo, C.-H. Tung, Y. Inoue, Y.-C. Liu, *J. Org. Chem.* **2002**, *67*, 2429–2434; d) Y.-H. Wang, Y. Fu, M.-Z. Zhu, X. Huang, Q.-X. Guo, *Res. Chem. Intermed.* **2003**, *29*, 11–19; e) Y.-H. Wang, M.-Z. Zhu, X.-Y. Ding, J.-P. Ye, L. Liu, Q.-X. Guo, *J. Phys. Chem. B* **2003**, *107*, 14087–14093; f) J. M. Haider, Z. Pikramenou, *Eur. J. Inorg. Chem.* **2001**, 189–194; g) M. J. J. P. Silva, J. M. Haider, R. Heck, M. Chavarot, A. Marsura, Z. Pikramenou, *Supramol. Chem.* **2003**, *15*, 563–571; h) J. M. Haider, R. M. Williams, L. De Cola, Z. Pikramenou, *Angew. Chem.* **2003**, *115*, 1874–1877; *Angew. Chem. Int. Ed.* **2003**, *42*, 1830–1833; i) J. M. Haider, Z. Pikramenou, *Chem. Soc. Rev.* **2005**, *34*, 120–132; j) A. McNally, R. J. Forster, N. R. Russell, T. E. Keyes, *Dalton Trans.* **2006**, *14*, 1729–1737; k) Q.-H. Wu, M.-Z. Zhu, S.-J. Wei, K.-S. Song, L. Liu, Q.-X. Guo, *J. Incl. Phenom. Macrocycl. Chem.* **2005**, *52*, 93–100; l) T. Liu, Y.-G. Wei, Q.-H. Wu, Q.-X. Guo, *Res. Chem. Intermed.* **2005**, *31*, 833–844; m) A. Quaranta, Y. Zhang, S. Filippone, J. Yang, P. Sinay, A. Rassat, R. Edge, S. Navaratnam, D. J. McGarvey, E. J. Land, M. Brettreich, A. Hirsch, R. V. Bensasson, *Chem. Phys.* **2006**, *325*, 397–403; n) S. K. Pal, T. Sahu, T. Misra, T. Ganguly, T. K. Pradhan, A. De, *J. Photochem. Photobiol. A* **2005**, *174*, 138–148; o) I. Hamachi, H. Takashima, Y.-Z. Hu, S. Shinkai, S. Oishi, *Chem. Commun.* **2000**, 1127–1128; p) J. M. Haider, M. Chavarot, S. Weidner, I. Sadler, R. M. Williams, L. De Cola, Z. Pikramenou, *Inorg. Chem.* **2001**, *40*, 3912–3921; q) J. A. Faiz, R. M. Williams, M. J. J. P. Silva, L. De Cola, Z. Pikramenou, *J. Am. Chem. Soc.* **2006**, *128*, 4520–4521.

[4] B. Balan, K. R. Gopidas, *Chem. Eur. J.* **2006**, *12*, 6701–6710.

[5] a) S. Tian, H. Zhu, P. Forgo, V. T. D'Souza, *J. Org. Chem.* **2000**, *65*, 2624–2630; b) A. R. Khan, P. Forgo, K. J. Stine, V. T. D'Souza, *Chem. Rev.* **1998**, *98*, 1977–1996.

[6] a) K. Harata, H. Uedaira, *Bull. Chem. Soc. Jpn.* **1975**, *48*, 375–378; b) H. Shimizu, A. Kaito, M. Hatano, *Bull. Chem. Soc. Jpn.* **1979**, *52*, 2678–2684; c) H. Shimizu, A. Kaito, M. Hatano, *Bull. Chem. Soc. Jpn.* **1981**, *54*, 513–519; d) M. Kodaka, *J. Phys. Chem.* **1991**, *95*, 2110–2112.

[7] a) M. Kodaka, *J. Phys. Chem. A* **1998**, *102*, 8101–8103; b) M. Kodaka, *J. Am. Chem. Soc.* **1993**, *115*, 3702–3705.

[8] a) J. W. Park, S. Y. Lee, H. J. Song, K. K. Park, *J. Org. Chem.* **2005**, *70*, 9505–9513; b) S. Hamai, T. Koshiyama, *J. Photochem. Photobiol. A* **1999**, *127*, 135–141; c) S. Pagliari, R. Corradini, G. Galaverna, S. Sforza, A. Dossena, M. Montalti, L. Prodi, N. Zaccheroni, R. Marchelli, *Chem. Eur. J.* **2004**, *10*, 2749–2758; d) R. P. Bonomo, S. Pedotti, G. Vecchio, E. Rizzarelli, *Inorg. Chem.* **1996**, *35*, 6873–6877; e) X. Zhang, W. M. Nau, *Angew. Chem.* **2000**, *112*, 555–557; *Angew. Chem. Int. Ed.* **2000**, *39*, 544–547; f) W. M. Nau, X. Zhang, *J. Am. Chem. Soc.* **1999**, *121*, 8022–8032; g) H. Takakusa, K. Kikuchi, Y. Urano, T. Higuchi, T. Nagano, *Anal. Chem.* **2001**, *73*, 939–942; h) T. Yorozu, M. Hoshino, M. Imamura, H. Shizuka, *J. Phys. Chem.* **1982**, *86*, 4422–4426; i) K. Kano, M. Hitoshi, Y. Yoshimura, S. Hashimoto, *J. Am. Chem. Soc.* **1988**, *110*, 204–209; j) A. Ueno, I. Suzuki, T. Osa, *J. Am. Chem. Soc.* **1989**, *111*, 6391–6397; k) M. A. Hossain, S. Matsumura, T. Kanai, K. Hamasaki, H. Mihara, A. Ueno, *J. Chem. Soc. Perkin Trans. 2* **2000**, 1527–1533; l) J. W. Park, H. E. Song, S. Y. Lee, *J. Phys. Chem. B* **2002**, *106*, 7186–7192.

[9] S. K. Chakrabarti, *Mol. Phys.* **1970**, *18*, 275–277.

[10] P. Jardon, R. Gautron, *J. Chim. Phys. Phys. Chim. Biol.* **1985**, *82*, 353–360.

[11] S. Fukuzumi, I. Nakanishi, K. Tanaka, *J. Phys. Chem. A* **1999**, *103*, 11212–11220.

[12] a) J. L. Sessler, C. T. Brown, D. O'Connor, S. L. Springs, R. Wang, M. Sathiosatham, T. Hirose, *J. Org. Chem.* **1998**, *63*, 7370–7374; b) A. Osuka, S. Marumo, Y. Wada, I. Yamazaki, T. Yamazaki, Y. Shirakawa, Y. Nishimura, *Bull. Chem. Soc. Jpn.* **1995**, *68*, 2909–2915; c) G. P. Wiederrecht, M. P. Niemczyk, W. A. Svec, M. R. Wasielewski, *J. Am. Chem. Soc.* **1996**, *118*, 81–91; d) T. Nagata, *Bull. Chem. Soc. Jpn.* **1991**, *64*, 3005–3016; e) S. C. Freilich, *Macromolecules* **1987**, *20*, 973–978.

 © 2007 Wiley-VCH Verlag GmbH & Co. KGaA, Weinheim

[13] Y. Matsushita, T. Suzuki, T. Ichimura, T. Hikida, *J. Phys. Chem. A* **2004**, *108*, 7490–7496.
[14] J. Gawroński, M. Brzostowska, K. Kacprzak, H. Kolbon, P. Skowronek, *Chirality* **2000**, *12*, 263–268.
[15] a) A. E. Kaifer in *Comprehensive Supramolecular Chemistry, Vol. 8* (Eds.: J. L. Atwood, J. E. D. Davies, D. D. MacNicol, F. Vögtle, J. A. Ripmeester), Pergamon, Oxford, **1996**, pp. 499–534; b) P. L. Boulas, M. Gümez-Kaifer, L. Echegoyen, *Angew. Chem.* **1998**, *110*, 226–258; *Angew. Chem. Int. Ed.* **1998**, *37*, 216–247.
[16] a) R. Isnin, C. Salam, A. E. Kaifer, *J. Org. Chem.* **1991**, *56*, 35–41; b) T. Matsue, D. H. Evans, T. Osa, N. Kobayashi, *J. Am. Chem. Soc.* **1985**, *107*, 3411–3417; c) A. Diaz, P. A. Quintela, J. M. Schuette, A. E. Kaifer, *J. Phys. Chem.* **1988**, *92*, 3537–3542.
[17] AM1 calculations of the molecular length were carried out using Titan Version 1 from Wavefunction Inc., 18401 Von Karman, Suite 370, Irvine, CA 92612.
[18] a) E. Prasad, K. R. Gopidas, *J. Am. Chem. Soc.* **2000**, *122*, 3191–3196; b) M. A. Smitha, E. Prasad, K. R. Gopidas, *J. Am. Chem. Soc.* **2001**, *123*, 1159–1165.
[19] a) D. Rehm, A. Weller, *Isr. J. Chem.* **1970**, *8*, 259–271; b) D. Rehm, A. Weller, *Ber. Bunsenges. Phys. Chem.* **1969**, *73*, 834–839.
[20] a) R. A. Marcus, P. Siders, *J. Phys. Chem.* **1982**, *86*, 622–630; b) P. Siders, R. A. Marcus, *J. Am. Chem. Soc.* **1981**, *103*, 741–747; c) R. A. Marcus, N. Sutin, *Biochim. Biophys. Acta* **1985**, *811*, 265–322; d) N. Sutin, *Acc. Chem. Res.* **1982**, *15*, 275–282; e) P. Suppan, *Top. Curr. Chem.* **1992**, *163*, 95–130, and references therein; f) S. Fukuzumi, M. Tanaka, M. Nishimine, K. Ohkubo, *J. Photochem. Photobiol. A 2005*, **175**, 79–88; g) S. Fukuzumi, M. Nishimine, K. Ohkubo, N. V. Tkachenko, H. Lemmetyinen, *J. Phys. Chem. B* **2003**, *107*, 12511–12518; h) P. A. Liddell, G. Kodis, D. Kuciauskas, J. Andréasson, A. L. Moore, T. A. Moore, D. Gust, *Phys. Chem. Chem. Phys.* **2004**, *6*, 5509–5515; i) L. R. Sutton, M. Scheloske, K. S. Pirner, A. Hirsch, D. M. Guldi, J.-P. Gisselbrecht, *J. Am. Chem. Soc.* **2004**, *126*, 10370–10381; j) D. I. Schuster, P. Cheng, P. D. Jarowski, D. M. Guldi, C. Luo, L. Echegoyen, S. Pyo, A. R. Holzwarth, S. E. Braslavsky, R. M. Williams, G. Klihm, *J. Am. Chem. Soc.* **2004**, *126*, 7257–7270.
[21] J. R. Lakowicz in *Principles of Fluorescence Spectroscopy*, Kluwer Academic, Dordrecht, **1999**.
[22] a) K. R. Gopidas, M. Bohorquez, P. V. Kamat, *J. Phys. Chem.* **1990**, *94*, 6435–6440; b) P. V. Kamat, J. P. Chauvet, R. W. Fessenden, *J. Phys. Chem.* **1986**, *90*, 1389–1394.
[23] a) J. Jortner, *J. Chem. Phys.* **1976**, *64*, 4860–4867; b) J. R. Miller, J. V. Bietz, R. K. Huddleston, *J. Am. Chem. Soc.* **1984**, *106*, 5057–5068.
[24] E. A. Weiss, E. T. Chernick, M. R. Wasielewski, *J. Am. Chem. Soc.* **2004**, *126*, 2326–2327.
[25] R. T. Hayes, C. J. Walsh, M. R. Wasielewski, *J. Phys. Chem. A* **2004**, *108*, 2375–2381.
[26] a) D. R. Worrall, S. L. Williams, F. Wilkinson, *J. Phys. Chem. B* **1997**, *101*, 4709–4716; b) R. Dabestani, J. Higgin, D. Stephenson, I. N. Ivanov, M. E. Sigman, *J. Phys. Chem. B* **2000**, *104*, 10235–10241; c) W. Li, M. A. Fox, *J. Phys. Chem. B* **1997**, *101*, 11068–11076.
[27] a) D. Mauzerall in *Photoinduced Electron Transfer, Part A* (Eds.: M. A. Fox, M. Channon), Elsevier, Amsterdam, **1988**, pp. 228–244; b) S. Fukuzumi, *Org. Biomol. Chem.* **2003**, *4*, 609–620; c) S. L. Segura, N. Martin, D. M. Guldi, *Chem. Soc. Rev.* **2005**, *34*, 31–47; d) T. E. Mallouk, P. G. Hoertz, *Inorg. Chem.* **2005**, *44*, 6828–6840; e) D. M. Guldi, H. Imahori, K. Tamaki, Y. Kashiwagi, H. Yamada, Y. Sakata, S. Fukuzumi, *J. Phys. Chem. A* **2004**, *108*, 541–548; f) H. Imahori, D. M. Guldi, K. Tamaki, Y. Yoshida, C. Luo, Y. Sakata, S. Fukuzumi, *J. Am. Chem. Soc.* **2001**, *123*, 6617–6628.
[28] S. Fukuzumi, H. Kotani, K. Ohkubo, S. Ogo, N. V. Tkachenko, H. Lemmetyinen, *J. Am. Chem. Soc.* **2004**, *126*, 1600–1601.
[29] S. L. Murov, I. Carmichael, G. L. Hug, *Handbook of Photochemistry*, Marcel Dekker, New York, **1993**, p. 293.
[30] a) I. Willner, B. Willner in *Frontiers in Supramolecular Organic Chemistry and Photochemistry* (Eds.: H.-J. Schneider, H. Dürr), VCH, Weinheim, **1991**, pp. 337–370; b) E. Adar, Y. Degani, Z. Goren, I. Willner, *J. Am. Chem. Soc.* **1986**, *108*, 4696–4700; c) N. Manoj, K. R. Gopidas, *Phys. Chem. Chem. Phys.* **1999**, *1*, 2743–2748.
[31] M. Tanaka, K. Ohkubo, C. P. Gros, R. Guilard, S. Fukuzumi, *J. Am. Chem. Soc.* **2006**, *128*, 14625–14633.
[32] B. O. Linn, L. M. Paege, P. J. Doherty, R. J. Bochis, F. S. Waksmunski, P. Kulsa, M. H. Fisher, *J. Agric. Food Chem.* **1982**, *30*, 1236–1242.
[33] N. K. Modukuru, K. J. Snow, B. S. Perrin, Jr., J. Thota, C. V. Kumar, *J. Phys. Chem. B* **2005**, *109*, 11810–11818.
[34] W. H. Melhuish, *J. Phys. Chem.* **1961**, *65*, 229–235.
[35] D. F. Eaton in *Handbook of Organic Photochemistry, Vol. 1* (Ed.: J. C. Scaiano), CRC Press, Boca Raton, FL, **2000**, p. 234.
[36] H. Lutz, E. Breheret, L. Lindqvist, *J. Phys. Chem.* **1973**, *77*, 1758–1762.
[37] R. Bensasson, E. J. Land, *Photochem. Photobiol. Rev.* **1978**, *3*, 163–191.
[38] I. Carmichael, G. L. Hug in *Handbook of Organic Photochemistry, Vol. 1* (Ed.: J. C. Scaiano), CRC Press, Boca Raton, FL, **2000**, p. 377.
[39] Y. Wang, J. J. Tria, L. M. Dorfman, *J. Phys. Chem.* **1979**, *83*, 1946–1951.

Received: December 7, 2006
Published online: March 28, 2007

 © 2007 Wiley-VCH Verlag GmbH & Co. KGaA, Weinheim